Influence of Shear Stress on In-Stent Restenosis: In Vivo Study Using 3D Reconstruction and Computational Fluid Dynamics

Marcelo Sanmartín,[a] Javier Goicolea,[b] Carlos García,[c] Javier García,[c] Antonio Crespo,[c] Javier Rodríguez,[d] and José M. Goicolea[d]

[a]Unidad de Cardiología Intervencionista, Hospital Meixoeiro, Vigo, Pontevedra, Spain.
[b]Unidad de Hemodinámica, Hospital Puerta de Hierro, Madrid, Spain.
[c]ESII, Grupo de Mecánica de Fluidos, Universidad Politécnica de Madrid, Madrid, Spain.
[d]ESIC, Grupo de Mecánica de Medios Continuos, Universidad Politécnica de Madrid, Madrid, Spain.

Introduction and objectives. Local factors may influence neointimal proliferation following conventional stent implantation. In this study, the relationship between wall shear stress and luminal loss after coronary stenting was assessed using a combination of angiography, intravascular ultrasound, and computational fluid dynamics.

Patients and methods. Seven patients with de novo right coronary lesions treated with conventional (i.e., bare metal) stents were included. Realistic three-dimensional geometric reconstructions were generated offline from angiographic and intravascular ultrasound data both immediately after stenting and at 6-month follow-up. A finite-volume model was used to calculate local wall shear stress within the stent and 4 mm proximally and distally to the stent. The mean coronary ostium entry flow velocity was assumed to be 25 cm/s in all cases.

Results. The mean neointimal thickness was 0.29 (0.21) mm. In 5 cases, weak negative correlations between wall shear stress and neointimal thickness were found: maximum r value $=-0.34$, minimum r value $= -0.11$ ($P<.001$). The neointimal thickness in segments in which the level of wall shear stress was in the lowest quartile was greater than that in segments in which it was in highest quartile, at 0.34 (0.21) mm and 0.27 (0.24) mm ($P<.001$) for quartiles 1 and 4, respectively.

Conclusions. Low wall shear stress after stenting favors neointimal proliferation both within the stent and at the stent's edges.

Key words: *Restenosis. Angioplasty. Intravascular ultrasound. Fluid dynamics.*

Influencia de la tensión de cizallamiento en la reestenosis intra-stent: estudio in vivo con reconstrucción 3D y dinámica de fluidos computacional

Introducción y objetivos. Los factores locales pueden influir en la proliferación neointimal tras la implantación de *stents* convencionales. En este estudio se evalúa la relación entre la tensión de cizallamiento y la pérdida luminal tras la colocación de *stents* en las arterias coronarias, utilizando la combinación de angiografía, ecografía intravascular y cálculo computacional de la dinámica de fluidos.

Pacientes y método. Se incluyó a 7 pacientes con lesiones *de novo* en las arterias coronarias derechas tratadas con *stents* convencionales (no recubiertos de fármacos). Se realizó una reconstrucción tridimensional real, basada en la angiografía y en la ecografía intracoronaria, realizada *offline* tras la angioplastia y a los 6 meses. Mediante el modelo de volúmenes finitos se calculó la tensión de cizallamiento localmente, en el interior del segmento con *stent* y en los 4 mm proximales y distales, tomando como velocidad de entrada en el *ostium* coronario un valor de 25 cm/s.

Resultados. El grosor neointimal medio fue de 0,29 ± 0,21 mm. En 5 casos se encontró una correlación negativa débil entre la tensión de cizallamiento y el grosor neointimal (valor máximo de r = –0,34, valor mínimo de r = 0,11; p < 0,001). Los segmentos en el cuartil inferior de la tensión de cizallamiento mostraron valores más altos de grosor neointimal, comparados con los del cuartil superior (0,34 ± 0,21 frente a 0,27 ± 0,24 mm; p < 0,001, para los cuartiles 1 y 4, respectivamente).

Conclusiones. La baja tensión de cizallamiento tras la implantación de *stents* convencionales favorece la pérdida luminal, tanto en los segmentos intra-*stent* como en los bordes del *stent*.

Palabras clave: *Reestenosis. Angioplastia. Ecografía intravascular. Fluidodinámica.*

INTRODUCTION

The reduction in lumen diameter that occurs following stent implantation is proportional to the extent of

ABBREVIATIONS

CFD: computational fluid dynamics.
IU: intravascular ultrasound.
NT: neointimal thickness.
WSS: wall shear stress.

vascular damage[1-4] and is also linked to a number of clinical and angiographic variables, such as diabetes, artery diameter, and the length of the lesion.[5] Although it has been suggested that low levels of wall shear stress (WSS) could favor the process of restenosis, it has been difficult to demonstrate such a relationship in humans. Given the role of shear stress in the composition and behavior of atherosclerotic plaques,[6-9] it is reasonable to assume that it may also be involved in proliferative responses following angioplasty.

Currently, direct calculation of flow velocity and pressure at the luminal surface is not possible in vivo. However, technological and scientific advances in mathematical and numerical models allows mathematical simulation of blood flow and the precise determination of local hemodynamic effects.[10] In this way, the WSS can be estimated in vivo and we can analyze the influence of hemodynamic variables on in-stent restenosis. Early studies using these methods yielded conflicting results. In 1 report, a negative correlation was suggested between WSS and neointimal proliferation following implantation of Wallstents,[11] while in another study no relationship was found between these 2 variables.[9]

The aim of this study was to assess the contribution of WSS to neointima formation following successful implantation of balloon-expandable stents. Realistic 3-dimensional (3D) geometric reconstruction was used based on a combination of conventional coronary angiography and IU alongside a technique for numerical simulation of blood-flow conditions known as computational fluid dynamics (CFD).

PATIENTS AND METHODS

Study Group

The study was approved by the local ethics committee and all patients signed an informed consent form. Inclusion criteria were as follows: patients should be at least 18 years old, present de novo lesions of less than 25 mm in length in native coronary arteries, and be considered candidates for treatment by angioplasty and stenting. Only proximal and medial segments of the right coronary artery were studied, in an effort to avoid complexities associated with large bifurcations such as that of the left main coronary artery. Exclusion criteria were as follows: intervention during the acute phase of myocardial infarction, substantial tortuosity proximal to the target lesion, severe calcification that could interfere with ultrasound analysis of the arterial edges, renal failure, anemia, significant systemic disease that could threaten life expectancy, and use of experimental devices or drugs for prevention of restenosis.

Angioplasty Procedures

Stent implantation was performed using a standard procedure. All patients were treated with aspirin and ticlopidine prior to the procedure. Unfractionated heparin (100 U/kg) was administered through the guide catheter. Prior to the introduction of the angioplasty guidewire, 2 angiographic projections of the target lesions were obtained and the artery was examined by intravascular ultrasound (IU). With the exception of patient 2, the stent was placed directly in all cases. The following stents were implanted: Multilink Ultra in 2 cases and Tetra in 2 cases (both from Guidant, Santa Clara, CA, USA); Jostent Flexmaster (Jomed, Ragendingen, Netherlands) in 1 case; and NIR (Boston Scimed, Natick, MA, USA) in 2 cases.

Imaging of the Coronary Arteries

In all cases, conventional angiography and IU were performed at baseline (following stent implantation) and at 6-month follow-up. Images were acquired using 6-French guide catheters following intracoronary administration of 200 μg nitroglycerin. Once satisfactory stent placement was achieved, 2 orthogonal projections were captured in DICOM format at a rate of 25 images per second, with the IU catheter positioned just beyond the distal edge of the stent. During capture of the angiographic images, contrast solution was injected following 1:1 dilution with saline in an effort not to obscure visualization of the IU catheter. Since identification of the edges of the intima was still possible, this allowed the trajectory of the catheter and anatomic markers such as side branches to be visualized at the same time. Images obtained in end-diastole were used for the geometric reconstruction. The trajectory of the IU catheter was used as the main axis or "backbone" with which to orientate the reconstruction of the transverse sections obtained by IU and, therefore, obtain a realistic 3D reconstruction.

Automated quantitative angiography data were obtained using a program available as part of the General Electric Advantx system (GE Medical Systems, Paris, France).

Conventional catheters (Atlantis 40 MHZ, Boston Scimed, San Jose, CA, USA) were used for IU. Ultrasound images were obtained digitally during ECG-triggered automated pullback using a specifically designed device (TomTec Imaging Systems, GMBH, Unterschleissheim, Germany). The system allowed correction for the

displacement of the intravascular-ultrasound catheter that occurs during the cardiac cycle and breathing, making it possible to obtain precise end-diastolic images for the longitudinal reconstruction.

Three-Dimensional Reconstruction and Generation of the Mesh

The technique used for reconstruction in this study was similar to that used by Slager et al.[12] Briefly, the technique is based on the superposition of ultrasound sections on the 3D trajectory of the coronary artery, or in this case, the IU catheter inside it. The ultrasound sections used were images obtained at intervals of 2 mm, with the first image taken 4 mm from the distal edge of the stent (most distal section) and the last section (most proximal) at the aorto-ostial junction. The lumen and external contours were manually identified and marked in each section. After marrying the line of the IU catheter obtained by angiography with the center of the ultrasound sections, the lumen and external contours were reconstructed perpendicularly at 2 mm intervals and the global geometry interpolated. Axial orientation of the ultrasound sections was performed by localization of 2 separate side branches identified both by angiography and IU.

Three-dimensional reconstruction allows generation of a virtual mesh that is used in the mathematical simulation of the fluid dynamics. The spatial reconstruction, segmentation (3D mesh), and fluid dynamic variables derived were obtained using specific software (Fluent, v. 6.0, Fluent Inc., Lebanon, NH, USA). Figure 1 shows an example of this kind of 3D reconstruction.

Computational Fluid Dynamics

A technique known as the finite volume method was used to calculate blood-flow conditions. The method is based on dividing the internal volume of the coronary artery into tiny parts or finite volumes (Figure 1).[13] Then, the Navier-Stokes equations are resolved, allowing the fluid-mechanical variables to be calculated for each of the elements. The application of this technique requires the construction of a mesh based on the reconstructed image of the coronary artery. The mesh process allows the vascular structure to be subdivided into finite volumes, in which the flow velocity and WSS can be calculated. In this study, the volume elements were hexahedrons with a mean resolution of 0.2 mm, such that each coronary artery was subdivided into a variable number of points in which the fluid-dynamic variables were calculated. The number of points varied according to the length and dimensions of the vessel studied.

For calculations of fluid dynamics it was assumed that blood behaved as a Newtonian fluid with a density of
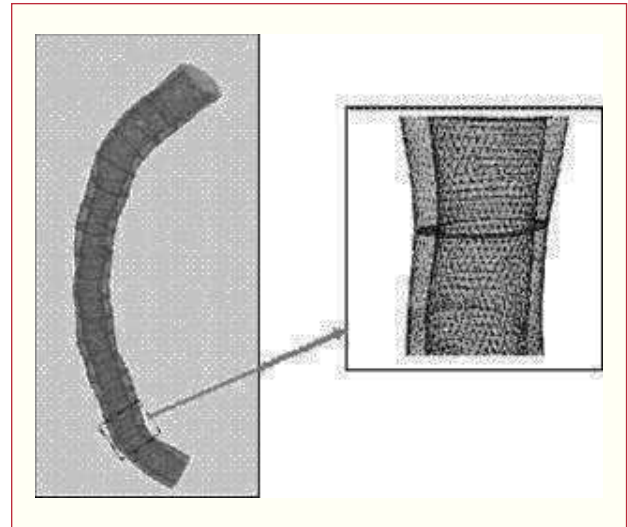

Figure 1. Example of a realistic 3D reconstruction used in the studies of fluid dynamics.

1050 kg/m^3 and a viscosity of 3 cP.[8,14] Laminar flow was assumed, taking into consideration the Reynolds number for a vessel with a diameter of between 3 and 4 mm. Variations in the cross-sectional area of the vessel during the cardiac cycle were not taken into account, since they are minimal in arteries that are atherosclerotic and, therefore, more rigid, and nonexistent in stented segments. Consequently, calculations were performed based on a fixed geometry for the luminal surface. The parabolic inflow velocity profile at the entrance of the coronary artery was taken to be 25 cm/s in all cases. This rate was chosen to simulate a situation at rest in all cases and is similar to the rate used in other studies.[8] The fluid dynamics were calculated in the stented sections at baseline (following expansion of the stent) and at 6-month follow-up.

Analysis and Statistics

Continuous variables are expressed as means (SD). Means were compared using the Student t test for independent samples. To assess the relationship between fluid dynamics and neointimal proliferation, an algorithm was developed specifically that allowed precise, robust correlation between the shear stress obtained from the CFD calculations and the local thickness of the vessel wall at each point.

In the segment studied, the internal mesh was obtained from the lumen contour of the IU performed at 6-month follow-up. The NT was calculated from the difference between that lumen contour and the stent contour. The thickness at the edges of the stent was obtained from the difference between the lumen contour at 6-month follow-up and that in the baseline condition following stent implantation. In this

TABLE 1. **Baseline Clinical Characteristics***

Patient	Age, Years	Sex	Diagnosis	Diabetes	Hypertension	Dyslipidemia	Smoking
1	57	Man	Recent MI	No	Yes	Yes	Yes
2	43	Man	Stable angina	No	No	No	No
3	63	Woman	Unstable angina	No	Yes	Yes	No
4	65	Man	Unstable angina	No	No	Yes	No
5	77	Man	Unstable angina	No	Yes	Yes	Yes
6	68	Man	Stable angina	No	Yes	No	Yes
7	49	Man	Recent MI	No	No	No	Yes

*MI indicates myocardial infarction.

TABLE 2. **Automated Quantitative Coronary Angiography of the Treated Segments***

Patient	Reference Diameter, mm	Baseline MLD, mm	Final MLD, mm	Length of the Lesion, mm	Length of the Stent, mm
1	2.9	1.1	2.8	21	18
2	3	0.4	2.9	10	58†
3	3	0.7	2.4	14.5	26
4	3	1.2	2	25	28
5	3.6	0.2	3.5	21	18
6	4	1.4	3.1	15	18
7	3.5	1.3	3.5	21	25

*MLD indicates minimum lumen diameter.
†In this case the stented segment includes the target lesion and the severely dissected proximal segment of the coronary artery.

calculation the edges included the 4 mm distal and proximal to the stent. Given the enormous number of points with data available from CFD, in order to be able to analyze correlations with wall thickness a specific algorithm was designed that allowed the number of points to be reduced and, at the same time, smoothed the data by eliminating undesirable local artifacts. To this end, a new interpolation mesh was constructed. Data with which to assess correlations between fluid dynamics and NT was available for an average of 2432 points (range, 955-5002) per coronary artery.

The relationship between shear stress and neointimal proliferation was assessed by linear regression analysis. Analysis of correlations was performed using the shear stress obtained at baseline. For a more accurate analysis of the fluid-dynamic conditions associated with restenosis, the shear stress was divided into quartiles. In this way, NT could be compared in different groups according to post-stent values for WSS.

Statistical calculations were performed using SPSS version 10.0. $P<.05$ was considered statistically significant.

RESULTS

The clinical and angiographic characteristics of the 7 patients included in the study are summarized in Tables 1 and 2. In all cases, it was possible to perform a 3D geometric reconstruction, both at baseline and follow-up. One patient required additional stents to cover a dissection proximal to the initial lesion that

extended up to the ostium of the coronary artery. Consequently, it was not possible to obtain the proximal edge without stent in this case. Figure 2 contains an example of a 3D reconstruction showing the estimated WSS and NT using a colored scale. Two patients presented angiographic restenosis (stenosis >50%) at follow-up and 1 of those patients required repeat angioplasty of the target lesion. In that case, IU was performed prior to dilatation.

NT and WSS

The mean NT in the treated segments, including the edges without the stent, was 0.29±0.21 mm and the WSS for the same segments was 1.93 Pa. In general, neointimal growth was greater in the segments covered by the stent than the in the edges (0.29±0.20 mm vs 0.14±0.31 mm; $P<.001$). In contrast, the WSS was significantly lower in the stented segments than the edges (1.82±1.10 Pa vs 2.40±2.10 Pa; $P<.001$).

Relationship Between Neointimal Proliferation and WSS

When all cases were considered, a weak negative correlation was observed between NT and WSS ($r=-0.15$; $P<.001$). The relationship between these 2 variables was similar in the stented segments and the edges, except in 1 case (Tables 3 and 4). A significant negative correlation between NT and WSS was observed in 5 patients. With the exception of 1 case,
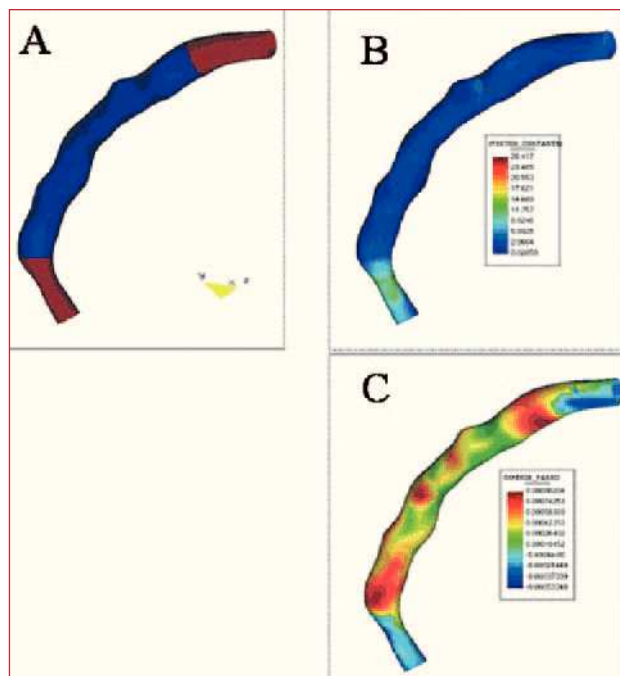
Figure 2. Example of a geometric reconstruction of the segment covered by the stent (shown in blue in panel A) and the proximal and distal edges (shown in brown in panel A). The wall shear stress and neointimal thickness are shown on a colored scale in panels B and C, respectively.

TABLE 3. Correlations Between NT and WSS in the Segments Studied*

Patient	r	Beta	95% CI	P
1	0.04	0.009	−0.01 to 0.019	.09
2	−0.33	−0.07	−0.076 to −0.065	<.001
3	−0.17	−0.018	−0.020 to −0.015	<.001
4	−0.26	−0.019	−0.022 to −0.016	<.001
5	−0.34	−0.035	−0.038 to −0.032	<.001
6	−0.04	−0.034	−0.082 to 0.012	.14
7	−0.11	−0.038	−0.050 to −0.026	<.001

*CI indicates confidence interval.

TABLE 4. Correlations Between NT and WSS. Data Obtained Within the Stent and at the Proximal and Distal Edges Analyzed Separately

Patient	In-Stent		Edges	
	r	P	r	P
1	0.01	.8	0.1	.02
2*	−0.32	<.001	−0.35	<.001
3	−0.21	<.001	−0.38	<.001
4	−0.22	<.001	−0.37	<.001
5	−0.36	<.001	−0.26	<.001
6	0.08	.02	−0.25	<.001
7	−0.26	<.001	0.27	<.001

*In this case, only the distal edge is included in the analysis.

the mean NT was significantly higher in the lower quartiles for WSS (Table 5). However, abnormally low values for WSS were recorded in that patient (Table 5). Grouping together all of the cases, in the quartiles corresponding to WSS the NT was 0.34±0.21 mm in quartile 1 and 0.27±0.24 mm in quartile 4 ($P<.0001$). The NT of the 4 groups for WSS is shown in Figure 3.

Evolution of WSS in Stented Segments

The baseline WSS in the stented segments shifted from 2.40±2.06 Pa to 3.43±3.26 Pa. This change in shear stress was positively correlated with the measured NT ($r=0.33$; $P<.0001$). Figure 4 shows the relationship between the change in WSS and the NT divided into quartiles. The mean increase in WSS for the lower and upper quartiles of NT was 0.22±1.80 Pa and 2.14±2.24 Pa, respectively ($P<.001$).

DISCUSSION

In this study, the influence of WSS on neointimal proliferation following intracoronary stent implantation was analyzed longitudinally in an in vivo human model. The main finding was a negative correlation between WSS and NT in 5 out of 7 cases studied. The lowest values for WSS were correlated with a higher degree of proliferation at 6 months. However, the observed correlation is weak and other,

more potent factors are certain to be involved in neointima formation.

Neointimal Proliferation Following Stent Implantation: the Role of Fluid Dynamics

Proliferation of scar tissue is practically the only mechanism of lumen loss following placement of stents.[1] The main trigger for this proliferative response is the mechanical stretching of the vessel wall, leading to the exposure of subendothelial structures to the blood flow and activation of a major thrombotic and inflammatory response.[4,5] The amount of neointimal tissue is proportional to the degree of damage caused, and local factors play a major role in the reparative response following angioplasty.[2,3] In fact, the presence of a metallic structure at the luminal surface contributes to the increased neointimal response[4,15] and even the design of the stent can influence this response.[16-18] Systemic variables, such as insulin resistance and diabetes can promote restenosis.[19] A correlation between restenosis and certain genetic polymorphisms has also been shown.[20-22]

Compared with other local factors, the role of fluid dynamics in neointimal proliferation has not been

TABLE 5. **Mean NT Following Division of the Shear Stress Into 4 Groups (Quartiles)***

Patient	Upper Limit of Q1 (Pa)	NT (Q1)	Lower Limit Q4 (Pa)	NT (Q4)	P
1	2.29	0.50±0.28	4.28	0.58±0.40	.003
2	1.08	0.32±0.18	1.84	0.20±0.11	<.0001
3	1.5	0.24±0.15	3.19	0.20±0.13	<.0001
4	0.94	0.49±0.18	2.29	0.34±0.20	<.0001
5	1.16	0.17±0.10	2.28	0.10±0.09	<.0001
6	0.5	0.33±0.19	0.78	0.31±0.16	.047
7	1.18	0.52±0.23	1.98	0.44±0.21	<.0001
All	1.11	0.34±0.21	2.35	0.27±0.24	<.0001

*Q1 indicates first quartile; Q4, fourth quartile.

extensively studied. The relationship between low WSS and progression of atherosclerosis can be inferred from the eccentric distribution of atherosclerotic plaques, which are generally thickest at the inner surface of curves in the arteries and the side opposing the flow division in bifurcations.[23,24]

In previous studies, numerical simulation of blood flow has shown a negative correlation between WSS and plaque progression[8]; however, the relationship is complex and is limited to certain patterns of vascular remodeling.[25] More recently, in an experimental model of angioplasty, Carlier et al[26] elegantly demonstrated that implantation of multiple flow dividers in an oversized stent placed in rabbit iliac arteries can attenuate neointimal growth and the inflammatory response. These findings suggest that hemodynamic conditions exert an influence on in-stent restenosis. However, the conclusions cannot be extrapolated directly to human models, since flow conditions, vascular geometry, and the extent of the response to lesions are very different.

Wentzel et al[11] used a similar 3D reconstruction model to the one employed here to evaluate 14 patients with Wallstents implanted in native coronary arteries. They demonstrated a negative correlation between NT and WSS in 9 patients. The *r* values varied between 0.04 and 0.65, with a beta coefficient of –0.08±10 mm. Although our findings are consistent with those of Wentzel et al, the impact of WSS on neointimal proliferation appears to be lower in our study. However, it is important to take into account certain methodological differences between the 2 studies. The results obtained with self-expanding stents such as the Wallstent are difficult to extend to balloon-expanded stents, which are in more widespread clinical use. Self-expanding stents generate a more intense neointimal response, partly due to the continued, late expansion.[16,17] Late expansion was not considered in the study of Wentzel et al, and the authors used the stent contour obtained at follow-up (generally considered to be larger than that measured immediately after implantation), possibly
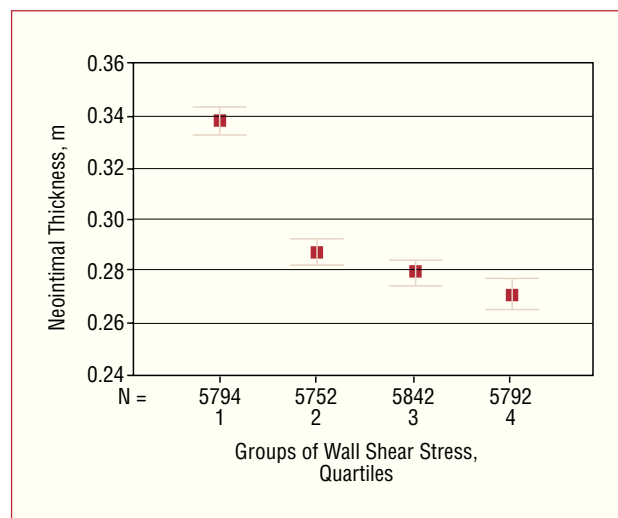
Figure 3. Distribution of neointimal thickness (y axis) according to wall shear stress divided into 4 groups (quartiles) shown on the x axis.
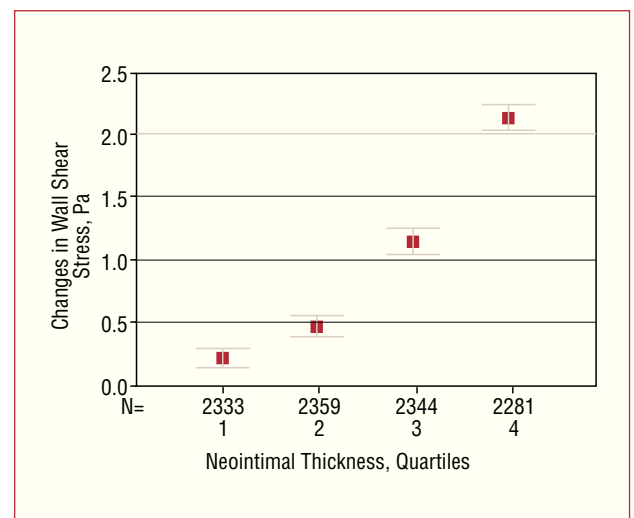
Figure 4. Changes in the wall shear stress (calculated as [value at follow-up]–[baseline value immediately after stent implantation]; y axis) in different groups (quartiles) of neointimal thickness (x axis).

leading to overestimation of the WSS at the luminal surface.

More recently, Stone et al[9] studied 6 coronary artery segments treated with conventional stents, also using numerical simulation of the fluid dynamic conditions and 3D reconstruction. While areas with low WSS were more prone to plaque accumulation and eccentric remodeling in sections not containing stents, there was no significant correlation between in-stent neointima formation and WSS. Again, certain methodological differences may explain these apparent discrepancies between our study and the results of Stone et al, such as the inclusion of branches of the left coronary artery, the methods used to estimate blood flow, and the segmentation of plaque thickness for analysis of correlations.

Our findings support the hypothesis that neointimal growth is correlated with flow conditions following stent placement. This relationship appears not to be present under conditions of physiologic or elevated of WSS. The correlation appears to be restricted to conditions of low shear stress and the pattern observed suggests a threshold effect on the proliferative response. The underlying cellular mechanisms could involve the activation of membrane receptors that are sensitive to conditions of reduced flow and that activate intracellular signals that favor the generation of neointimal tissue. The outcome would be normalization of flow conditions at the vessel wall through growth into the lumen of the artery. In fact, in our study, estimation of the WSS over time revealed an exponential increase in those areas with greatest neointimal growth (Figure 4). It should be noted that the 2 cases in which no correlation was observed between baseline fluid dynamic conditions and neointimal proliferation showed the highest and lowest absolute values, with limited changes along the length of the stent (patients 1 and 6, respectively; Table 5). This finding is also suggestive of a threshold for shear stress beyond which the stimulus for proliferation of the tissue is triggered.

Finally, we were able to analyze the behavior at the edges of the stent, areas in which the greatest loss often occurs following angioplasty. The results suggest a similar role for fluid dynamics at this site, with a weak negative correlation between WSS and lumen loss.

Implications

These findings further support the general recommendation that good, uniform expansion is ensured in segments treated with stents. Nevertheless, the implications of this study in terms of restenosis in the currently available drug-eluting stents are unclear, since those stents generate almost no neointimal response.

Limitations

The main limitation of this study is the small number of cases included, justified by the overall complexity of the procedure. Nevertheless, the large number of points and the wide range of shear stress values analyzed for each coronary artery lessen this limitation. None of the coronary arteries studied had significant tortuosity or bifurcations, and furthermore, the results of angioplasty in terms of stent expansion could be considered satisfactory, without clear areas of underexpansion, which can prevent assessment of these specific conditions. However, the mathematical simulation of fluid dynamics in a tortuous vessel is difficult using these methods because the geometric reconstruction is based on a central axis obtained from the IU catheter and the presence of the device stretches the artery, neutralizing the natural curves observed by angiography.

Finally, the fact that we did not perform a direct assessment of flow velocity prevents estimation of the absolute values of WSS. However, the calculations are based on values for the velocity that are commonly seen in the right coronary artery and allow temporal changes in the WSS to be analyzed in the same artery.

CONCLUSIONS

The present study shows a negative correlation between WSS and neointimal proliferation. However, the influence of this fluid dynamic variable appears to be limited and, furthermore, is restricted to conditions of reduced flow. The implications of these findings for the current use of drug-eluting stents are unclear.

REFERENCES

1. Mintz GS, Popma JJ, Hong MK, Pichard AD, Kent KM, Satler LF, et al. IU to discern device-specific effects and mechanisms of restenosis. Am J Cardiol. 1996;78:1822.
2. Schwartz RS, Huber KC, Murphy JG, Edwards WD, Camrud AR, Vlietstra RE, et al. Restenosis and the proportional neointimal response to coronary artery injury: results in a porcine model. J Am Coll Cardiol. 1992;19:267-74.
3. Hoffmann R, Mintz GS, Mehran R, Kent KM, Pichard AD, Satler LF, et al. Tissue proliferation within and surrounding Palmaz-Schatz is dependent on the aggressiveness of stent implantation technique. Am J Cardiol. 1999;83:1170-4.
4. Edelman ER, Rogers C. Pathobiologic responses to stenting. Am J Cardiol. 1998;81:E4-6.
5. Bauters C, Isner J. The biology of restenosis. In: Topol EJ, editor. Textbook of cardiovascular medicine. Philadelphia: Lippincot-Raven; 1998. p. 2465-89.
6. Gibson CM, Díaz L, Kandarpa K, Sacks FM, Pasternak RC, Sandor T, et al. Relation of vessel wall shear to atherosclerosis progression in human coronary arteries. Atheroscler Thromb. 1993;13:310-5.
7. Dirksen M, van der Wal A, van der Berg FM, van der Loos CM, Becker AE. Distribution of inflammatory cells in atherosclerotic

plaques relates to the direction of flow. Circulation. 1998;98: 2000-3.

8. Krams R, Wentzel JJ, Oomen JA, Schuurbiers JC, Andhyiswara I, Kloet J, et al. Evaluation of endothelial shear stress and 3D geometry as factors determining the development of atherosclerosis and remodeling in human coronary arteries in vivo. Combining 3D reconstruction from angiography and IVUS (ANGUS) with computational fluid dynamics. Arterioscler Thromb Vasc Biol. 1997;17:2061-5.

9. Stone PH, Coskun AU, Kinlay S, Clark ME, Sonka M, Wahle A, et al. Effect of endothelial shear stress on the progression of coronary artery disease, vascular remodeling, and in-stent restenosis in humans. In vivo 6-month follow-up study. Circulation. 2003;108:438-44.

10. Goicolea Ruigómez JM. Factores biomecánicos y su influencia en la función cardiovascular. Rev Esp Cardiol. 2005;58:121-5.

11. Wentzel JJ, Krams R, Schuurbiers JC, Oomen JA, Kloet J, van der Giessen WJ, et al. Relationship between NT and shear stress after wallstent implantation in human coronary arteries. Circulation. 2001;103:1740-5.

12. Slager CJ, Wentzel JJ, Schuurbiers JC, Oomen JA, Kloet J, Krams R, et al. True 3-dimensional reconstruction of coronary arteries in patients by fusion of angiography and IVUS (ANGUS) and its quantitative validation. Circulation. 2000;102:511-6.

13. Eric W. Weisstein. "Finite Volume Method". From MathWorld-A Wolfram Web Resource. Available from: http://mathworld.wolfram.com/FiniteVolumeMethod.html.

14. Joshi AK, Leask RL, Myers JG, Ojha M, Butany J, Ethier RS. Intimal thickness is not associated with WSS patterns in the human right coronary artery. Arterioscler Thromb Vasc Biol. 2004;24:2408-13.

15. Serruys PW, de Jaegere P, Kiemeneij F, Macaya C, Rutsch W, Heyndrickx G, et al. A comparison of balloon-expandable stent implantation with balloon angioplasty in patients with coronary artery disease: Benestent Study Group. N Engl J Med. 1994;331:489-95.

16. Sanmartín M, Goicolea J, Alfonso F, Escaned J, Flores AA, Fernández-Ortiz A, et al. Implicaciones de la expansión tardía de los stents autoexpandibles sobre la respuesta neointimal: estudio seriado con ecografía intravascular. Rev Esp Cardiol. 2002;55:16-24.

17. von Birgelen C, Airiian SG, de Feyter PJ, Foley DP, van der Giessen WJ, Serruys PW. Coronary wallstents show significant late, posprocedural expansion despite implantation with adjunct high-pressure balloon inflations. Am J Cardiol. 1998;82:129-34.

18. Escaned J, Goicolea J, Alfonso F, Pérez-Vizcaíno MJ, Hernández R, Fernández-Ortiz A, et al. Propensity and mechanisms of restenosis in different coronary stents designs. Complementary value of the analysis of the luminal gain-loss relationship. J Am Coll Cardiol. 1999;34:1490-7.

19. Aronson D, Bloomgarden Z, Rayfield EJ. Potential mechanisms promoting restenosis in diabetic patients. J Am Coll Cardiol. 1996;27:528-35.

20. Amant C, Bauters C, Bodart JC, Lablanche JM, Grollier G, Danchin N, et al. D allele of the angiotensin I-converting enzyme is a major risk factor for restenosis after coronary stenting. Circulation. 1997;96:56-60.

21. Ribichini F, Steffenino G, Dellavalle A, Matullo G, Colajanni E, Camilla T, et al. Plasma activity and insertion/deletion polymorphism of angiotensin I-converting enzyme: a major risk factor and a marker of risk for coronary stent restenosis. Circulation. 1998;97:147-54.

22. Koch W, Mehilli J, von Beckerath N, Böttiger C, Schömig A, Kastrati A. Angiotensin I-converting enzyme (ACE) inhibitors and restenosis after coronary artery stenting in patients with the DD genotype of the ACE gene. J Am Coll Cardiol. 2003;41: 1957-61.

23. Fuster V, Badimon L, Badimon JJ, Chesebro JH. The pathogenesis of coronary artery disease and the acute coronary syndromes. N Engl J Med. 1992;326:242-50.

24. Kimura BJ, Russo RJ, Bhargava V, McDaniel MB, Peterson KL, deMaria AN. Atheroma morphology and distribution in proximal left anterior descending artery: in vivo observations. J Am Coll Cardiol. 1996;27:825-31.

25. Wentzel JJ, Janssen E, Vos J, Schuurbiers JCH, Krams R, Serruys PW, et al. Extension of increased atherosclerotic wall thickness into high shear stress regions is associated with loss of compensatory remodeling. Circulation. 2003;108:17-23.

26. Carlier SG, van Damme LCA, Blommerde CP, Wentzel JJ, van Langehove G, Verheye S, et al. Augmentation of WSS inhibits neointimal hyperplasia after stent implantation. Inhibition through reduction of inflammation? Circulation. 2003;107:2741-6.